Paper

Phase Conjugate Image Enhancement using Photorefractive Media and Application to Surface Defect Detection

Member Takashi Kuroiwa (Nihon University)
Member Tsuneki Yamasaki (Nihon University)
Member Mitsuhito Matsubara (Nihon University)

Phase conjugation has recently represented a new technique for optical measurement. However, the optical intensity of phase conjugate images is weak because the phase conjugate generation efficiency of photorefractive media is relatively low. In this paper, we have proposed a new method for enhancing the phase conjugate image, and have discussed the quality of output images both experimentally and theoretically, based on diffraction and propagation theories. The successful application of the presented method to surface defect detection demonstrates the effectiveness and applicability of this new technique in this field.

Keywords: Photorefractive media, $BaTiO_3$ crystal, surface defect, phase conjugate wave, beam amplification

1. Introduction

Photorefractive media have been recognized as optical devices that can be used for phase conjugate wave generation and beam amplification, and have recently been applied to optical measurement, optical image processing and optical computing (1)~(4).

As a practical example, if the phase conjugation is applied to optical image measurement, the output image contains very limited aberration. Moreover, as a lens system is unnecessary, it is likely that small measuring devices will be realized based on this technology.

However, the phase conjugate generation efficiency of photorefractive crystals is relatively low. Therefore, the optical intensity of the output image is also weak (5)(6), and it is desirable to increase the intensity of these images. However, the research on this problem hardly has been reported.

In this study, we propose an image enhancement technique by using photorefractive two-wave mixing in order to increase the intensity of phase conjugate images. We also applied the technique to surface defect detection as a demonstration of practical application, and it is shown that the technique is very effective.

In this paper, the enhancement technique for phase conjugate images based on photorefractive two-wave mixing is examined, followed by an examination of blur in the enhanced image which is made both by an experimental and theoretical approach based on diffraction and propagation theory of light. A surface defect on a low-reflectivity sample is then detected using the proposed method.

2. Optics configuration for phase conjugate image enhancement

We consider a schematic diagram of the experimental setup for phase conjugate image enhancement as shown

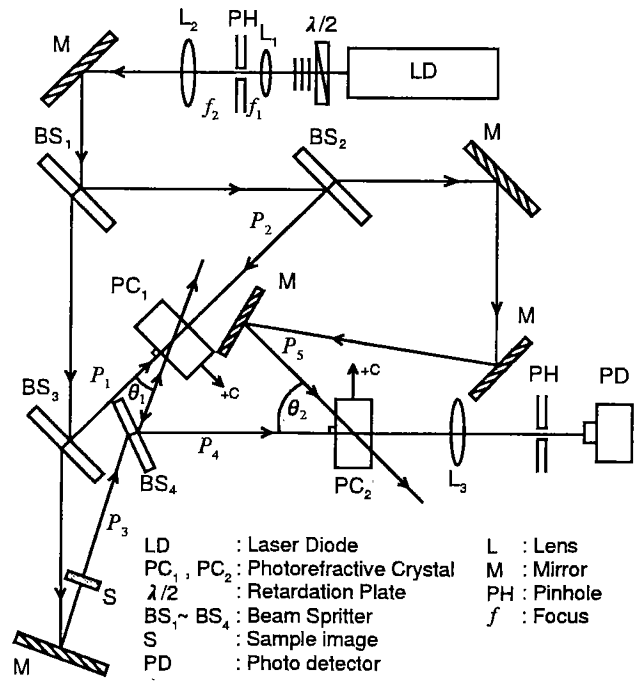

Fig. 1. Experimental setup for the phase conjugate image enhancement

in figure 1. A laser diode (LD) is used as the light source (wavelength 532 [nm]), and the plane of polarization is leveled using a half-wave retardation plate (7). A four-wave mixing of counter-propagating pump geometry is used to generate the phase conjugate wave. P_1 and P_2 are forward and backward pump beams, respectively, and P_3 is the probe beam. PC_1 and PC_2 are photorefractive $BaTiO_3$ crystals ($5 \times 5 \times 3$ [mm]). The phase conjugate image generated by crystal PC_1 enters the crystal PC_2 at the input plane, and the image is amplified by two-wave mixing (P_4 is used as the signal beam, and P_5 is the pump beam). The distance from the beam splitter BS_4 to the input plane of the crystal PC_2 is equal to the distance from the BS_4 to the image pattern S. The size of the image pattern S was made to be under half of the size of the crystal PC_2 and the large aperture lens L_3 was used in order to reduce a blur in image enhancement. The incident angles are $\theta_1 = 20$[deg] and $\theta_2 = 50$[deg]. The focal distance of lenses L_1, L_2 and L_3 are $f_1 = 30$ [mm], $f_2 = 170$ [mm] and $f_3 = 60$ [mm], respectively. Pinhole PH is used in order to reduce the scattered light.

3. Enhancement of phase conjugate image

We examine the amplification by photorefractive two-wave mixing for the weak intensity of the phase conjugation wave, the experiment is performed with the lenses L_1, L_2, and L_3 and image patterns S removed from the optical system, as shown in figure 1.

The time variation of the phase conjugate output $P_4(0,t)$ and the amplification output $P_4(L,t)$ are shown in figure 2. The figure reveals that the amplification output $P_4(L,t)$ is rapidly increased by 300 [sec]. The remarkable change over 300 [sec] of the amplification output is not observed and the output is almost 15 times of the phase conjugate output $P_4(0)$. When the incidence intensity ratio m $(=P_5(0)/P_4(0))$ is 1000; $P_4(0)$ is the phase conjugate power near the input plane of the crystal PC_2, and is constant output value as the time passed through over 10 seconds. $P_5(0)$ is the pump beam power near the input plane of the crystal PC_2 and it does not change with the time.

The relationship between the gain g $(=P_4(L)/P_4(0))$ and the incidence intensity ratio m is shown in figure 3, The gain g increases with the incidence intensity ratio m; $P_4(L)$ is the power of the amplification output near the exit plane of the crystal PC_2, and is the value as the amplification output becomes constant. In this case, the output value as the time passed through over 300 [sec] is used. L is the crystal length. In the experiment, the measured value changes by the effect of the slight vibration from the circumference of the experimental apparatus. Therefore, the mean value of many measured values is shown in the figure 3. The dots in figure are the measured values, and the solid curve is the calculated value by using the coupled–mode equation [8]. The experimental result agrees with the calculation result comparatively.

From the results in figure 2 and 3, it is verified that the phase conjugate output can be sufficiently amplified using the photorefractive two-wave mixing.

The result in amplifying the phase conjugation image is shown in figure 4. The phase conjugate image that is not emphasized is shown in figure 4(a). The image is measured by the CCD camera in the position where the phase conjugate image is reproduced and the crystal PC_2 and lens L_3 are removed from the optical system. Although the edges in the image can be recognized, the intensity of the image is weak. The enhanced image is shown in figure 4(b). The image is measured by putting the CCD camera in the position where it is reproduced at the size equal to the enhanced image. The optical intensity of the enhanced image is about 10 times of the intensity of the phase conjugate image. The blur of the image is small, and the remarkable difference compared with figure 4(a) is not observed.

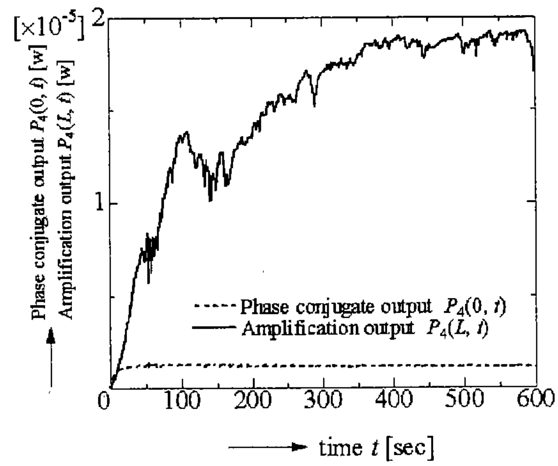

Fig. 2. Temporal variation of amplification output

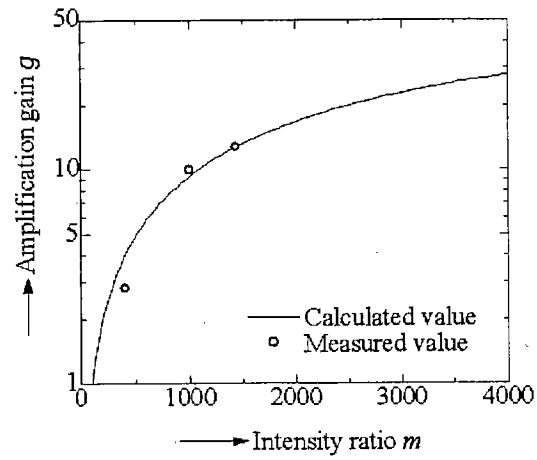

Fig. 3. Incident intensity ratio dependence of the amplification gain

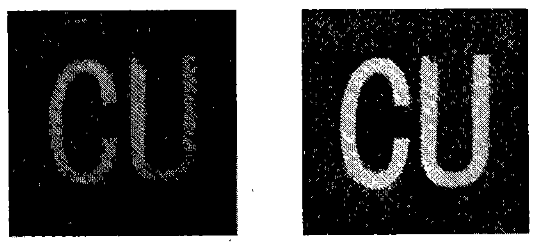

(a) Phase conjugate image (b) Enhanced image

Fig. 4. Phase conjugate image and enhanced image

4. Examination on blur in enhanced image

We investigate the blur of the enhanced image both experimentally and theoretically based on diffraction and propagation theory. The analytical model for the image reproduction system is shown in figure 5. If the probe beam P_3, containing the image information, propagates distance L_p in the z direction, the high-order diffracted light is lost because the crystal PC_1 has a finite aperture. In addition, the high-order diffracted light of the input image (phase conjugate image) are lost via the aperture of crystal PC_2 when the input image is enhanced by two-wave mixing. The image reproduced on the Z_s plane is blurred by the apertures of the two crystals.

Here, the z axis is defined as the propagation direction of the probe beam P_3 and phase conjugate wave P_4, and the x axis is perpendicular to these two beams. The analyzed image is assumed to be unidimensional. The image distribution $A_p(x, z_t)$ on the plane of crystal PC_1 is given in the following equation [9]:

$$A_p(x,z_t) = \sqrt{\frac{j}{\lambda L_p}} \exp(-jkL_p) \times \int_{-\infty}^{\infty} A_p(x_p, z_p) \exp\left\{-jk\frac{(x-x_p)^2}{2L_p}\right\} dx_p \quad (1)$$

where $A_p(x, z_p)$ is the light amplitude distribution of the input image pattern on Z_p plane, λ is wavelength, L_p is the distance from the image pattern S to the crystal PC_1, and k is the wave number ($= 2\pi/\lambda$) in vacuum.

The image distribution $A_c^*(x, z_t)$ of phase conjugate wave generated by crystal PC_1 on the Z_t plane is given by

$$A_c^*(x,z_t) = RA_p(x,z_t) rect\left(\frac{2x}{D_c}\right) \quad \cdots\cdots\cdots\cdots (2)$$

where R is the phase conjugate generation efficiency of the phase conjugate wave, D_c is the aperture of the phase conjugate mirror which is equal to the height of crystal PC_1 (= 5 mm), and $rect(x)$ is defined as

$$rect(x) = \begin{cases} 1 & (x \leq 1) \\ 0 & (x > 1). \end{cases} \quad \cdots\cdots\cdots\cdots (3)$$

The image distribution $A_c^*(x, z_t)$ comes to $A_c^*(x, z_p)$ when it reaches the Z_p plane:

$$A_c^*(x,z_p) = \sqrt{\frac{j}{\lambda L_p}} \exp(jkL_p) \times \int_{-\infty}^{\infty} A_c^*(x_t, z_t) \exp\left\{jk\frac{(x-x_t)^2}{2L_p}\right\} dx_t. \cdot (4)$$

The image from the Z_p plane is enhanced by two-wave mixing in the crystal PC_2, the image distribution comes to $A_c^*(x, z_\ell)$ on the Z_ℓ plane in which the aperture plane of lens L_3 is located:

$$A_c^*(x,z_\ell) = \sqrt{\frac{j}{\lambda L_1}} \exp\left\{jk\left(L_1 + \frac{x^2}{2L_1}\right)\right\} \times F\left\{\sqrt{g}A_c^*(x_p,z_p) rect\left(\frac{2x}{D_c}\right) \exp\left(jk\frac{x_p^2}{2L_1}\right)\right\} \times \exp\left\{-jk\frac{x^2}{2f}\right\} P(x) \quad \cdots\cdots\cdots (5)$$

where, $F\{\cdot\}$ means Fourier transform, and x_p is the variable used for the transform, g is the amplification gain, D_c is the height of the crystal PC_2 (= 5 [mm]), and $P(x)$ is the function of the entrance pupil of the lens. If lens aberration is neglected, we can describe the function by the equation [10]

$$P(x) = rect\left(\frac{2x}{D_\ell}\right). \quad \cdots\cdots\cdots\cdots (6)$$

Therefore, the image distribution $A_c^*(x, z_s)$ on the Z_s plane is given by

$$\begin{aligned} A_c^*(x,z_s) &= \sqrt{\frac{j}{\lambda L_2}} \exp\left\{jk\left(L_2 + \frac{x^2}{2L_2}\right)\right\} \times F\left\{A_c^*(x_\ell,z_\ell) \exp\left\{jk\frac{x_\ell^2}{2L_2}\right\}\right\}_{f=\frac{x_\ell}{\lambda L_2}} \\ &= -\frac{1}{M} \exp\left\{jk\left(L_1 + L_2 + \frac{x^2}{2L_2}\right)\right\} \times \left\{\sqrt{g}A_c^*\left(-\frac{x}{M}, z_p\right) rect\left(-\frac{2x/M}{D_c}\right) \times \exp\left(jk\frac{x^2}{2ML_2}\right) \otimes \bar{P}\left(\frac{x}{\lambda L_2}\right)\right\} \quad \cdots (7) \end{aligned}$$

where x_ℓ is the variable used for the transform, M is magnification ($= L_2/L_1$), and $a \otimes b$ means the convolution operation of a and b. $\bar{P}(x)$ is given by

$$\bar{P}(x) = D_\ell sinc\left(D_\ell\frac{x}{\lambda L_2}\right) = \frac{sin(D_\ell x/\lambda L_2)}{x/\lambda L_2}. \quad (8)$$

In the following analysis, the blur of the output image is examined using equation (7).

When the unidimensional input image is given, as shown in figure 6(a), the intensity distribution of the output image is calculated using equation (7). The calculation is performed with $\lambda = 532[nm]$, $L_p = 250[mm]$, $L_1=L_2=120$[mm], $D_c = 5[mm]$, and $D_\ell = 60[mm]$.

The intensity distribution of the output image is shown in figure 6(b), and is obtained by dividing the range $|x| \leqq 1$[mm] into 256 equal parts and calculating the intensity at each point. As shown in this figure, the output image exhibits a gradient of the intensity distribution at the edges of the image. Therefore, the enhanced image is blurred compared with the input image.

The enhanced image obtained experimentally, shown in figure 7(b), is blurred compared to the input image (fig. 7(a)). The intensity ration m is 1000 in order to obtain the sufficient amplification gain. The intensity distribution of the image in figure 7(c) is obtained by

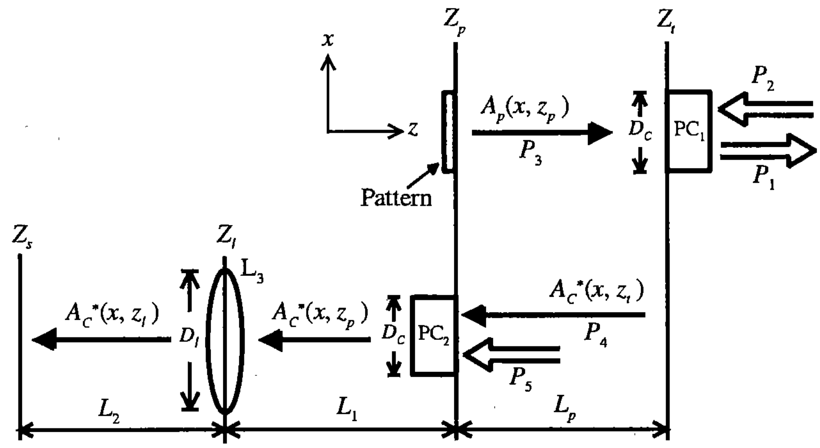

Fig. 5. The model of the image reproduction system

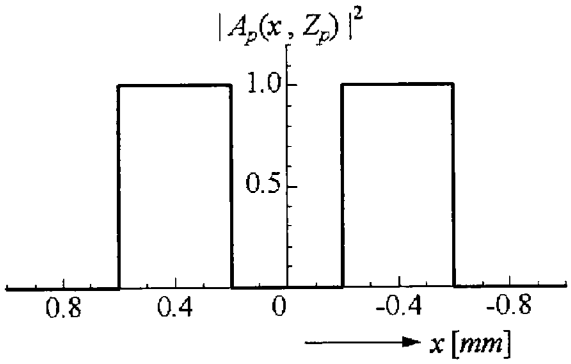

(a) Input image

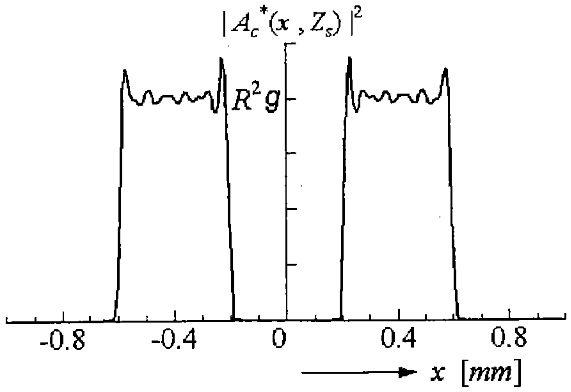

(b) Output image

Fig. 6. Intensity distribution of images obtained by the calculation

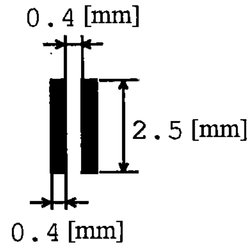

(a) Input image

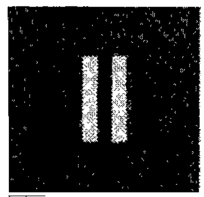

(b) Output image (m=1000)

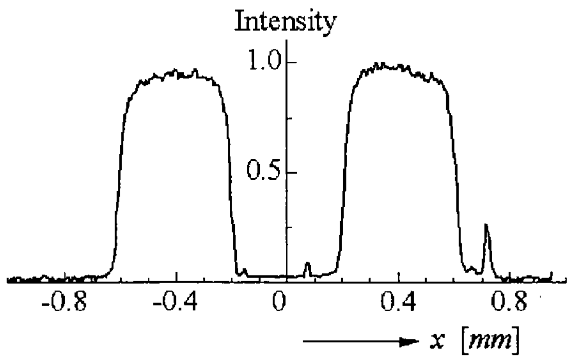

(c) Output image (The case of unidimensional scanning)

Fig. 7. Intensity distribution of images obtained by the experiment

unidimensional scanning of the intensity distribution of the output image at the width of a pixel in the direction of line width and converting the intensity distribution into digitized value, it is normalized at the maximum value of the intensity. A peak appears at around $x = 0.7$ [mm] which is generated by scattered light or multiple reflection between the lens and the CCD camera. The experimental result agrees well with the calculation result.

5. Application to surface defect detection

We examine the effectiveness of the presented method to surface defect detection. The defect is measured using the experimental setup shown in figure 1. In this case, the reflected light from the inspection object is used as the probe beam. The inspection object is put in the position used instead of the mirror M between

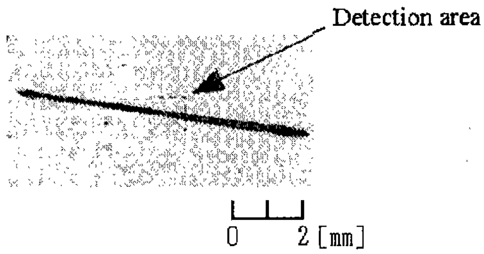

Fig. 8. Surface defect on the silicon wafer

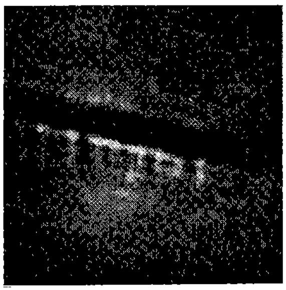

(a) The image before enhancement

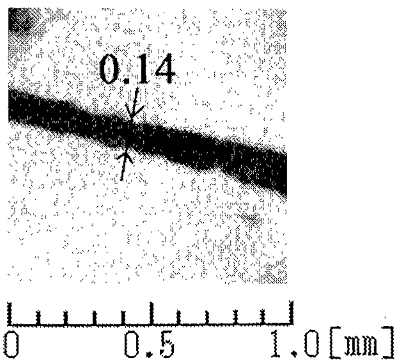

(b) Enhanced image

Fig. 9. The image of surface defect

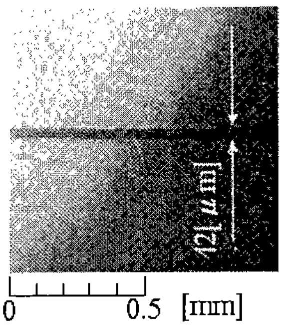

Fig. 10. Surface defect on the black acrylic sheet

beam splitter BS_3 and BS_4, and image pattern S is removed. The enhanced defect image is expanded at 2 times in the lens L_3 and is photographed by CCD camera. The surface defect used in this experiment is a scratch on a silicon wafer, as shown in figure 8. The detection area is 1×1[mm], and the line width of the scratch is about 0.14 mm. The phase conjugate image before enhancement is shown in figure 9(a); though the surface defect can be recognized, the intensity of image is weak. The enhanced image is shown in figure 9(b); the surface defect can be easily recognized.

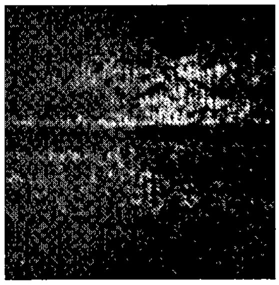

(a) The image before enhancement

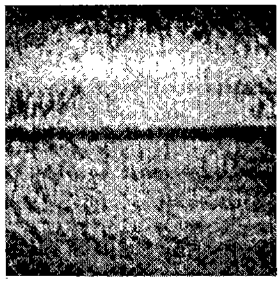

(b) Enhanced image

Fig. 11. The image of surface defect

The surface defect detection of the black acrylic sheet, in which the reflectivity is lower than the silicon wafer, is examined. A surface defect(a scratch) on a black acrylic sheet is shown in figure 10. The detection area is 1×1[mm] and the line width of the scratch is about 40[μm]. The non-enhanced image is shown in figure 11(a). The intensity of image is weak. The enhanced image is shown in figure 11(b). The scratch can be easily recognized. In addition, the image is accurately reproduced as the shape of the scratch. From these results, it is demonstrated that the small defect can be easily measured by the presented method and the technique is effective.

6. Conclusion

In this paper, we have proposed new method for enhancing phase conjugate images based on two-wave mixing. The results of both experiments and calculations demonstrated the following: (1) This method provides sufficient enhancement of phase conjugate images, (2) Blur of the enhanced output image was clarified from experimentally and theoretically based on diffraction and propagation theory, (3) Application of the presented method to surface defect detection confirmed that small defects can be easily recognized and accurately measured, and the surface defect image with the sufficient intensity is obtained even when the reflectivity of the object under inspection is low.

It is concluded that a simple real–time surface defect detection system may be realized using the presented method.

Acknowledgments

The authors wish to thank Professor T. Hinata, Professor T. Hosono and Professor K. Kawanishi for their

continued guidance.

(Manuscript received January 29, 2001, revised December 28, 2001)

References

(1) P. Günter, and J.P.Huignard, Photorefractive Materials and Their Applications II, Springer-Verlag, Berlin, 1989.
(2) P. Yeh, and C. Gu, ed., Landmark Papers on Photorefractive Nonlinear Optics, World Scientific Publ., 1995.
(3) P. Günter, ed., Nonlinear Optical Effects and Materials, Springer-Verlag, Berlin, 2000.
(4) F. T. S. Yu, and S. Yin, Photorefractive Optics, Academic Press, 2000.
(5) M. Matsubara, T. Katsuragawa, and H.Yamada, Measurement of surface defect by optical phase conjugation, J. of JSNDI, 9, 442(1991).
(6) M. Matsubara, T. Katsuragawa, and H.Yamada, Measurement of surface defects and fingerprint pattern by optical phase conjugate wavefront, ITEJ Tech. Rep., 13, 33(1991).
(7) T. Kuroiwa, A. Yamase, and M. Matsubara, Beam Amplification by Degenerate Two-Wave Mixing in Photorefractive Crystals, Proc. 1997 Elec. Soc. Conf. of IEICE, C-4-33, 281(1997).
(8) P. Yeh, Introduction to Photorefractive Nonlinear Optics, Wiley, 1993.
(9) A. Okamoto, S. Kunihiro, T. MISHIMA, and I. SAKURABA, Image Reconstruction Characteristic of Phase Conjugator via Nearly Degenerate Four-Wave Mixing, Trans. IEICE, J76-C-I, 7, 277(1993).
(10) K. Iizuka, Optical Enfineering, Kyoritsu Publ., 1983.
(11) J. Sakai, Phase Conjugate Optics, Asakura Publ., 1990.
(12) T. Kuroiwa and M. Matsubara, Selective Image Amplification by Two-Wave Mixing with Two Photorefractive $BaTiO_3$ Crystals, Trans. IEICE, J82-C-1, 9, 537(1999).
(13) T.Kuroiwa, M.Tsutsumi, and M.Matsubara, The Amplification of Phase Conjugate Image by Degenerate Two-Wave Mixing, Proc. 1999 Elec. Soc. Conf. of IEICE, C-4-11, 238(1999).
(14) T.Kuroiwa, M.Tsutsumi, and M.Matsubara, Amplification of Image of Surface Defect Using Two-Wave Mixing, Proc. 2000 IEICE General Conf., C-4-25, 373(2000).
(15) T.Kuroiwa, M.Tsutsumi, T.Yamasaki, and M.Matsubara, Study on the Picture Quality in the Phase Conjugate Image Enhancement Using Two-Wave Mixing, Proc. 2000 Elec. Soc. Conf. of IEICE, C-4-10, 281(2000).
(16) T. Kuroiwa, T. Yamasaki, and M. Matsubara, Development of surface defect measurement using photorefractive media, OFSET2000, 381(2000)

Takashi Kuroiwa (Member) received his B.E. and M.E. degrees in the Department of Precision Mechanical Engineering from Nihon University in 1987 and 1989, respectively. He received his Ph.D. degree (specializing Electrical Engineering) from Nihon University in 1995. In that year, he became a part-time Lecturer of Department of Electrical Engineering. In 1997, he works in the Nihon University, as a Reserch Assistant from 1997 to 2000. In 2001, he is an Assistant Professor at Nihon University. He has been engaged in research on control theory, network theory, electromagnetic theory and nonlinear optics.

Tsuneki Yamasaki (Member) received the B. E. degree from College of Industrial Technology, Nihon University in 1975, and M. S. and D. E. degree from College of Science and Technology, Nihon University in 1977 and 1986, respectively. He joined College of Science and Technology, Nihon University as a Research Assistant from 1977 to 1986 and was promoted to an Assistant Professor in 1987 and to an Associate Professor in 1991,and became a Professor at the Junior College, Nihon University, Dept. of Industrial Technology in 1997.Since 2000,he has been a Professor at the College of Science and Technology, Nihon University, Dept. of Electrical Engineering. He was a Visiting Scientist at MIT, Cambridge, USA, on leave of absence from Nihon University, from September 1989 to September 1990. His research interests are in the scattering and guiding problems of electromagnetic waves. Dr. Yamasaki received the Research Encouragement Award for young scientist from the Institute of Electronics, Information and Communication Engineers (IEICE), Japan in 1985.

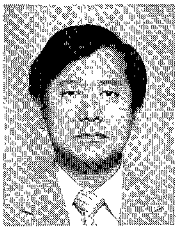

Mitsuhito Matsubara (Member) received his B.S. and M.S. degrees in the Department of Electrical Engineering from Nihon University in 1971 and 1973, respectively. He received his Ph.D. degree in Electrical Engineering from Nihon University in 1978. In that year, he works in the Nihon University. In 1992, he became a Professor at Nihon University. He has been engaged in study of magneto-optical recording, conduction of heat in amorphous rare earth-transition metal films, pattern processing, real–time holography and nonlinear optics. He has co-author of Electromagnetics for Engineering (Corona Publ.).